



Cite this: *Chem. Sci.*, 2025, **16**, 5503

All publication charges for this article have been paid for by the Royal Society of Chemistry

Received 16th December 2024  
Accepted 4th February 2025

DOI: 10.1039/d4sc08484e

[rsc.li/chemical-science](http://rsc.li/chemical-science)

## Introduction

Plastics possess many significant advantages such as light weight, low cost, easy processability, and tunable properties, enabling their widespread applications as diverse as packaging, construction materials, electronics, and energy storage.<sup>1–3</sup> As a result, plastics have become the largest synthetic consumer product in the world with an annual production of over 400 million tons.<sup>4,5</sup> However, only around 9% of all plastics have been recycled,<sup>6</sup> which means most of the used plastics are discarded unintentionally or intentionally. The inert characteristics endow plastics with useful material properties, which also make them resistant to degradation under ambient conditions with an estimated lifetime of over hundreds of years.<sup>7</sup> Plastic waste in the soil not only hinders the sustainable use of land,

but also reduces nutrients and contaminates water absorbed by crops.<sup>8</sup> Additionally, the discarded plastics in the oceans also threaten the survival of aquatic animals, which would potentially invade the human food chain.<sup>9</sup>

Degradable plastics, especially biodegradable plastics, have recently attracted much attention in both industrial and academic realms. The superb strategy is to create chemically degradable polymer materials for dynamically achieving depolymerization and reformation.<sup>10–16</sup> Improving legitimate measures to increase the collection of discarded plastics is the prerequisite for realizing a closed-loop recyclable process. Another approach is to promote the development of biodegradable plastics such as polyesters through the degradation of plastics with enzymes secreted by microorganisms in the environment.<sup>17</sup> However, efficient biodegradation is only observed in fertile soil with plenty of enzymes,<sup>18</sup> still resulting in the fast accumulation of plastics under common environmental conditions. Hence, developing robust plastics with minimal environmental burdens is highly desired for mitigating the negative consequences of plastics.

Ions are ubiquitous and concentrated in diverse natural environments such as seawater and soil, mainly including  $\text{Na}^+$ ,  $\text{K}^+$ ,  $\text{SO}_4^{2-}$ , and  $\text{Cl}^-$ .<sup>19,20</sup> Coincidentally, most of the discarded plastics mainly enter the oceans and soils, giving rise to both visual and ecological pollution.<sup>21</sup> If plastics can be efficiently decomposed with the assistance of ions in the environment, the issues caused by the discarded plastics would be readily

<sup>a</sup>Hefei National Research Center for Physical Sciences at the Microscale, Department of Chemical Physics, Key Laboratory of Surface and Interface Chemistry and Energy Catalysis of Anhui Higher Education Institutes, University of Science and Technology of China, Hefei, Anhui, 230026, China. E-mail: [gml@ustc.edu.cn](mailto:gml@ustc.edu.cn)

<sup>b</sup>The Key Laboratory of Functional Molecular Solids, Ministry of Education, Department of Materials Chemistry, School of Chemistry and Materials Science, Anhui Normal University, Wuhu, Anhui, 241002, China. E-mail: [zanhua23@ahnu.edu.cn](mailto:zanhua23@ahnu.edu.cn)

<sup>†</sup> Electronic supplementary information (ESI) available: Experimental details,  $^1\text{H}$  NMR spectra, UV-Vis spectra, FT-IR spectra, TGA, X-ray photoelectron spectroscopy, dynamic light scattering, scanning electron microscopy and mechanical properties of supramolecular polyelectrolyte plastics. See DOI: <https://doi.org/10.1039/d4sc08484e>



resolved. Unfortunately, conventional plastics are highly hydrophobic and stable under ambient conditions with diverse ions.<sup>22</sup> Hydrophilic polymers or networks usually undergo uncontrolled dissolution/swelling under aqueous conditions regardless of ions.<sup>23,24</sup> Simultaneously, the presence of common ions usually plays a trivial role in either surface or bulk degradation of current degradable plastics. Recently, salt-bridging of sodium hexametaphosphate with di- or tritopic guanidinium sulfate in water has been used to form a cross-linked supramolecular network, which is stable unless electrolytes are resupplied.<sup>25</sup> However, the complex design of the ionic monomer limits its widespread application. Therefore, it is highly challenging to fabricate readily available plastics that are robust and stable but can spontaneously dissociate under natural environments with common ions.

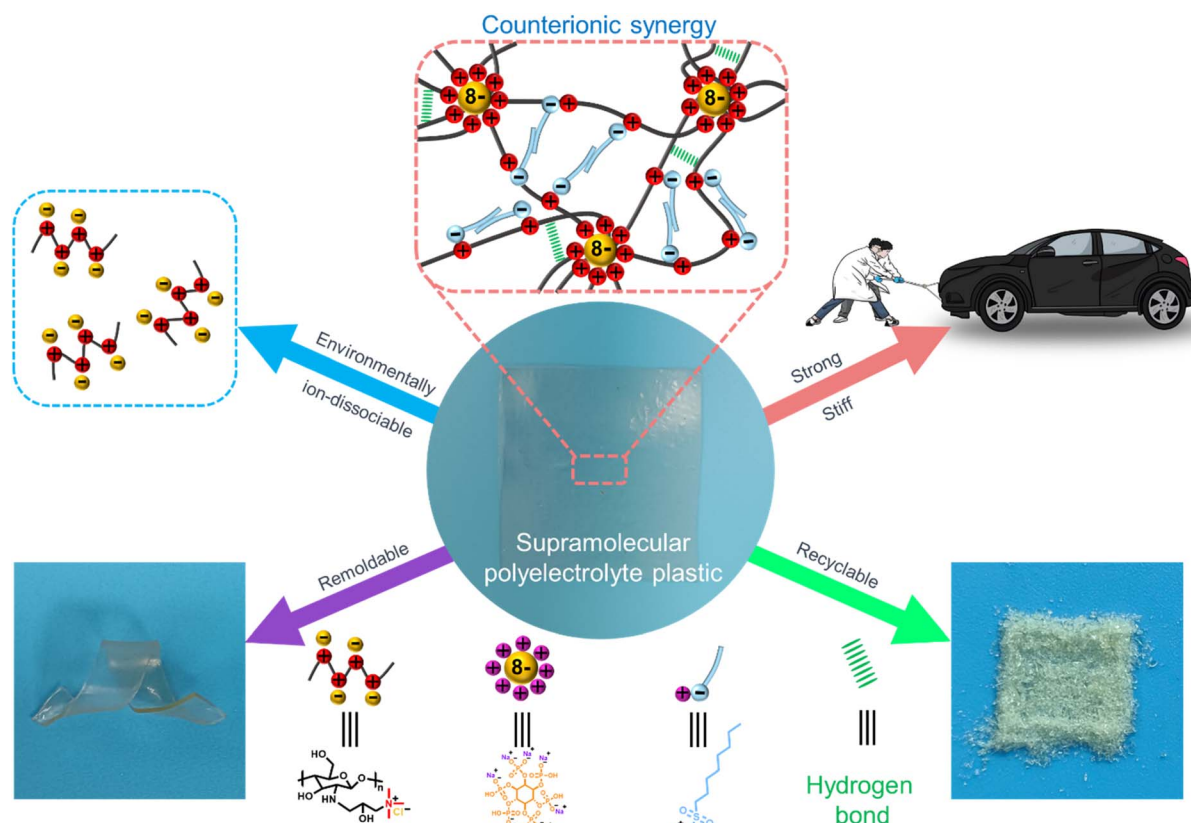
Herein, we develop an efficient method to construct high-performance supramolecular polyelectrolyte plastics with environmentally ion-dissociable properties. As a demonstration, hydroxypropyl trimethyl ammonium chloride chitosan (HACS-Cl) as a bio-sourced cationic polyelectrolyte was upgraded into supramolecular plastics through counterion exchange with multivalent sodium phytate (SP) and hydrophobic sulfonates. HACSs with only monovalent hydrophobic sulfonates have moderate mechanical properties, which were synergistically enhanced by combining multivalent and hydrophobic counterions. The obtained polyelectrolyte plastics with dynamic supramolecular hydrogen bonding and multiple electrostatic

crosslinking were further stabilized through hydrophobic interactions (Scheme 1). The unique dynamic network structures endow polyelectrolyte plastics with excellent remoldability, good recyclability, and efficient dissociation in seawater and soil under ambient conditions. Meanwhile, eco-friendly polyelectrolyte plastics have outstanding mechanical properties with a maximum tensile strength of  $93.6 \pm 3.3$  MPa and a maximum Young's modulus of  $2.3 \pm 0.3$  GPa, surpassing most of the commercial plastics. The simple strategy based on counterion exchange of polyelectrolytes developed herein is a universal route to producing robust sustainable polyelectrolyte plastics. These findings offer us a feasible way for fabricating environmentally ion-dissociable high-performance supramolecular polyelectrolyte plastics in a straightforward manner.

## Results and discussion

### Properties of HACS with different monovalent counterions

Chitin is the second most abundant biopolymer, following cellulose, and is derived from natural resources such as the shells of crabs, shrimps, insects, etc. As one of the important derivatives of chitin, HACS-Cl has low toxicity, good biocompatibility, and high water solubility,<sup>26</sup> possessing good processability and potential applicability as a bio-based feedstock. The abundant hydroxyl groups in HACS-Cl enable the formation of a strong supramolecular hydrogen bonding network, but



**Scheme 1** Schematic diagram of the fabrication of environmentally ion-dissociable high-performance supramolecular polyelectrolyte plastics with a synergistic multivalent and hydrophobic counterion strategy.



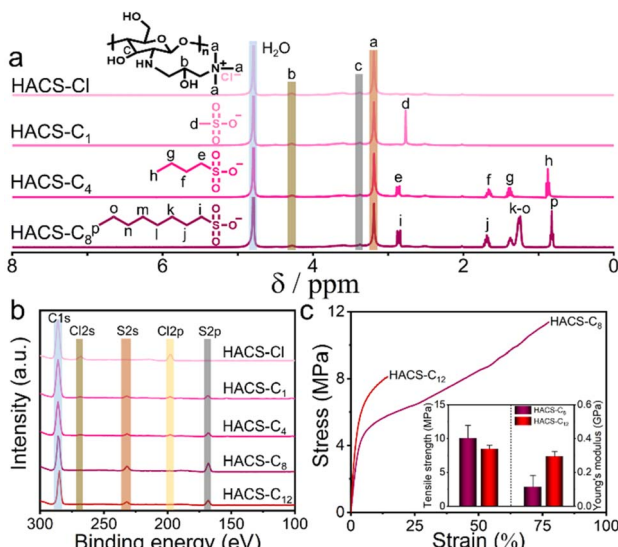


Fig. 1 Characterization of cationic polyelectrolytes HACSs with different monovalent counterions. (a) <sup>1</sup>H NMR spectra and (b) XPS analyses of HACS-Cl and HACS-C<sub>x</sub> materials. (c) Representative stress-strain curves for HACS-C<sub>8</sub> and HACS-C<sub>12</sub> with the inset showing the tensile strengths and Young's moduli.

uncontrolled hydration in the presence of water or high humidity hinders its application as a material with stable and robust mechanical properties. Of note, the pendant quaternary ammonium group provides an excellent means to modulate the material's properties by treating HACS-Cl as a type of strong cationic polyelectrolyte.

The positively charged HACS-Cl is supposed to exhibit a relatively weak interaction between the pendant quaternary ammonium group and the counterion – chloride ion (Cl<sup>-</sup>) – according to the Law of Matching Water Affinities (LMWA).<sup>27-29</sup> As a result, the properties of HACS-Cl can be tuned by introducing diverse counterions that interact more strongly with the pendant quaternary ammonium groups. Sulfonates with different lengths of hydrophobic chains, including sodium methanesulfonate, sodium 1-butanesulfonate, sodium 1-octanesulfonate, and sodium laurylsulfonate, were initially utilized for the counterion exchange to generate HACS-C<sub>1</sub>, HACS-C<sub>4</sub>, HACS-C<sub>8</sub>, and HACS-C<sub>12</sub>, respectively. The HACS-Cl aqueous solution was mixed with aqueous solutions containing different sulfonates and the obtained mixtures were further dialyzed against water to yield the targeted product. The counterion exchange for HACS-Cl was analyzed by using <sup>1</sup>H nuclear magnetic resonance (NMR) spectroscopy (Fig. 1a). Both the peak at 3.19 ppm for the methyl group of HACS-Cl and the peak at around 2.84 ppm for the alkyl group of the sulfonates have been observed for a series of HACS-C<sub>x</sub> materials with different alkyl groups of the sulfonates. These results suggest the successful exchange of counterions. Notably, HACS-C<sub>12</sub> has a too long hydrophobic chain, preventing its solubility in deuterated water for NMR analysis.

Further, the counterion exchange of HACS-Cl was investigated through X-ray photoelectron spectroscopy (XPS). XPS analyses show that the peaks for Cl 2s and Cl 2p become weak or

even disappear and the peaks for S 2s and S 2p emerge for all HACS-C<sub>x</sub> materials (Fig. 1b). The quantitative calculations of the relative elemental contents illustrate that the counterion exchange ratio between Cl<sup>-</sup> and sulfonates gradually increases from 75% for HACS-C<sub>1</sub> to nearly 100% for HACS-C<sub>12</sub> with the increasing length of the alkyl chain (Table S1†). These results can be rationalized according to the LMWA, since the more weakly hydrated alkyl sulfonate anions with longer alkyl chains tend to more strongly bind to the weakly hydrated quaternary ammonium groups in HACS-Cl driven by counterion exchange. Additionally, the counterion exchange of HACS-Cl also enhances the thermal stability of the polymers from the thermogravimetric analysis (TGA) results (Fig. S1†). The initial HACS-Cl has a relatively low decomposition temperature of 166.5 °C, which might be caused by Cl-catalyzed thermolysis. With the replacement of Cl<sup>-</sup> with sulfonates, high decomposition temperatures over 236.9 °C were observed for all HACS-C<sub>x</sub> materials, demonstrating good application potential.

Interestingly, stable polyelectrolyte plastics HACS-C<sub>8</sub> and HACS-C<sub>12</sub> can be obtained from the hydrophilic polyelectrolyte HACS-Cl through counterion exchange. Both HACS-C<sub>1</sub> and HACS-C<sub>4</sub> polyelectrolyte plastics with relatively weak hydrophobic interactions are observed to be still highly soluble in water, preventing their applications as stable polymeric materials. The mechanical properties of HACS-C<sub>8</sub> and HACS-C<sub>12</sub> were evaluated through stress-strain tests (Fig. 1c). The tensile strengths of HACS-C<sub>8</sub> and HACS-C<sub>12</sub> are 10.0 ± 1.8 MPa and 8.5 ± 0.5 MPa with the Young's moduli of 0.1 ± 0.07 GPa and 0.3 ± 0.03 GPa, respectively, as shown in the inset of Fig. 1c. The moderate mechanical properties of HACS-C<sub>8</sub> and HACS-C<sub>12</sub> are comparable to those of common bio-based plastics from plant oils or itaconic acids (Fig. S2†), but it is still desired to fabricate robust bio-based plastics outperforming commercial plastics for expanding their practical applications. We suppose that the hydrophobic interactions introduced by counterion exchange are not strong enough to enhance the supramolecular network of HACS-Cl for robust mechanical properties.

### Robust mechanical properties of supramolecular polyelectrolyte plastics with a synergistic multivalent and hydrophobic counterion strategy

The stiffness of polymeric materials is usually improved by increasing the covalent crosslinking density through the incorporation of multifunctional crosslinkers. Yet, the dense covalent polymer networks often give rise to the uncontrollable recyclability and poor degradation of relevant materials. We set out to use reversible multivalent electrostatic interactions for the fabrication of robust polymeric materials. SP as a bio-based small molecule from plant seeds has hexaphosphate groups capable of electrostatically crosslinking the polyelectrolyte HACS-Cl. Indeed, a white precipitate of HACS-SP was observed when mixing the SP solution with the HACS-Cl solution at pH ~ 7 (Fig. S3†). Proper negative charge and hydration of SP are necessary for the formation of crosslinked polyelectrolytes. The low negatively charged SP could not form efficient electrostatic interactions with the cationic HACS-Cl under the acidic



conditions at pH  $\sim$  2, and the high hydration of SP under the basic conditions at pH  $\sim$  12 hinders its efficient binding with the weakly hydrated quaternary ammonium groups in HACS-Cl (Fig. S3†).

As shown in Fig. 2a, XPS analysis of HACS-SP shows that the peaks at 189.0 eV and 133.0 eV respectively for P 2s and P 2p appear and the peak at 197.4 eV for Cl 2p decreases concomitantly, in comparison with the XPS data of HACS-Cl. Meanwhile, the supramolecular polyelectrolyte plastic HACS-SP presents a much higher tensile strength of  $37.6 \pm 0.7$  MPa than  $10.0 \pm 1.8$  MPa for HACS-C<sub>8</sub>. Both results illustrate the successful crosslinking of HACS-Cl with the introduction of multivalent SP. Further analysis of the XPS result indicates that only 66.2% of the Cl<sup>-</sup> was exchanged in HACS-SP (Table S2†). This might be caused by the steric hindrance effect, limiting the accessibility of Cl<sup>-</sup> for the counterion exchange by the multivalent SP. In order to further improve the mechanical and hydrophobic properties of HACS-SP through counterion exchange, monovalent sulfonates, including sodium 1-butanesulfonate, sodium 1-octanesulfonate, and sodium laurylsulfonate with different hydrophobic chains, were added to produce HACS-SP-C<sub>4</sub>, HACS-SP-C<sub>8</sub>, and HACS-SP-C<sub>12</sub>, respectively. It is found that the residual Cl<sup>-</sup> can be further exchanged with monovalent sulfonates, showing over 93% exchange of the Cl<sup>-</sup> (Fig. 2a and Table S2†).

Importantly, the strengths of the supramolecular polyelectrolyte plastics manifest synergistic enhancement with the combination of multivalent and hydrophobic counterions. Specifically, the tensile strengths of HACS-SP-C<sub>4</sub>, HACS-SP-C<sub>8</sub>, and HACS-SP-C<sub>12</sub> are  $55.8 \pm 1.3$ ,  $93.6 \pm 3.3$ , and  $54.7 \pm 2.4$  MPa, respectively (Fig. 2b and c). Simultaneously, the Young's moduli represent the same trend with a maximum value of  $2.3 \pm 0.3$  GPa for HACS-SP-C<sub>8</sub>. Both the tensile strengths and Young's moduli of

HACS-SP-C<sub>x</sub> materials are better than the sum of the values for HACS-SP and HACS-C<sub>x</sub> materials at the relative molar ratio content of SP and C<sub>x</sub> in HACS-SP-C<sub>x</sub> materials, demonstrating the synergistic effect of multivalent and hydrophobic counterions. With the introduction of hydrophobic counterions into the HACS-SP network, the obtained HACS-SP-C<sub>x</sub> materials strengthen the hydrophobic interactions, giving rise to the improvement of mechanical properties. Meanwhile, we have used scanning electron microscopy (SEM) to study the fracture behaviors during the tensile test. Interestingly, the polyelectrolyte plastic shows a smooth extension crack path, exhibiting a brittle fracture (Fig. S4†). Polyelectrolyte plastics are inclined to form highly dense structures attributed to strong electrostatic interactions. We suppose that polyelectrolyte plastics display strong interfacial bonding through synergistic multivalent and hydrophobic interactions, contributing to high stiffness. When the hydrophobic sulfonates change from sodium 1-butanesulfonate to sodium laurylsulfonate, attenuated total reflectance Fourier transform infrared (ATR-FTIR) results of HACS-SP-C<sub>x</sub> materials illustrate that the longer hydrophobic alkyl chain is able to more strongly disrupt the supramolecular hydrogen bonding network of HACS-Cl (Fig. S5†). As a result, outstanding mechanical properties were achieved for the supramolecular polyelectrolyte plastic HACS-SP-C<sub>8</sub>. Meanwhile, the notched HACS-SP-C<sub>8</sub> can still maintain the same Young's modulus, displaying a high fracture energy of  $10.3 \text{ kJ m}^{-2}$  (Fig. S6†).

The obtained supramolecular polyelectrolyte plastic HACS-SP-C<sub>8</sub> displays outstanding tensile strength and Young's modulus, outperforming many commercial petroleum-sourced, bio-based,<sup>11,30–34</sup> epoxy, phenolic resin and polyelectrolyte plastics (Fig. S7†), such as low/high-density polyethylene (PE), polypropylene (PP), polystyrene (PS), poly(vinyl chloride) (PVC),

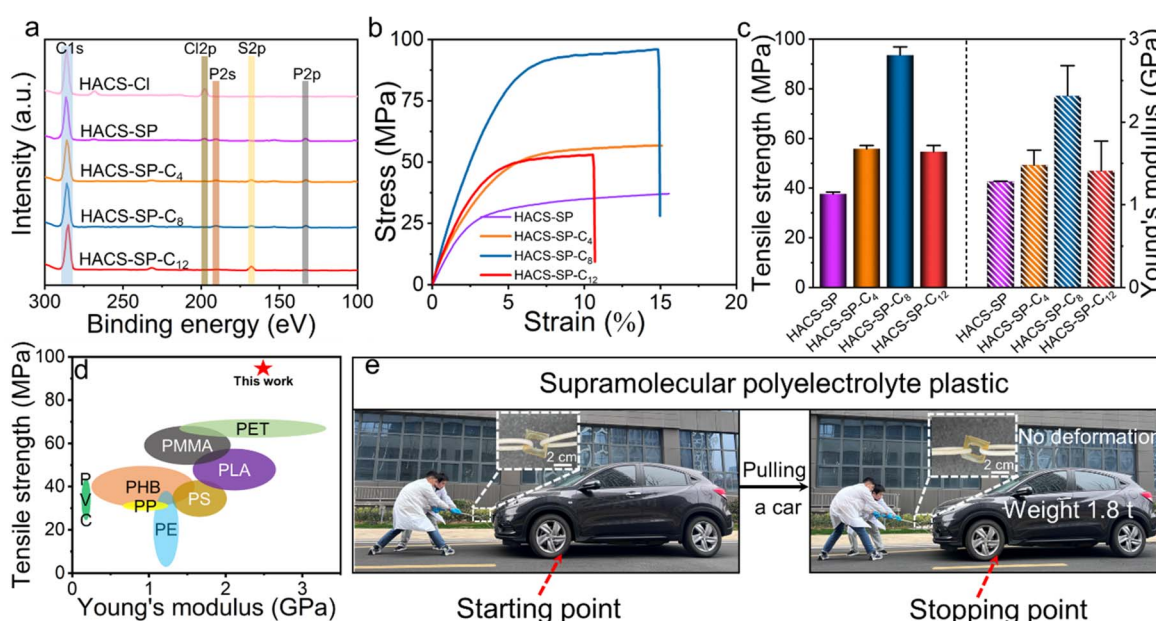


Fig. 2 Mechanical properties of supramolecular polyelectrolyte plastics. (a) XPS analyses, (b) representative stress–strain curves, and (c) mechanical properties of supramolecular polyelectrolyte plastics HACS-SP and HACS-SP-C<sub>x</sub> materials. (d) Comparison of the mechanical properties of the supramolecular polyelectrolyte plastic HACS-SP-C<sub>8</sub> with common plastics. (e) The demonstration of the strong and stiff HACS-SP-C<sub>8</sub> plastic by pulling a car over 1.8 tonnes.



poly( $\beta$ -hydroxybutyrate) (PHB), and polylactic acid (PLA) (Fig. 2d). It is even better than engineering plastics,<sup>30,35</sup> such as poly(methyl methacrylate) (PMMA) and poly(ethylene terephthalate) (PET) (Fig. 2d). In addition, HACS-SP-C<sub>8</sub> also has good flexibility and transparency (Fig. S8 and S9†). Good chemical stability of the supramolecular HACS-SP-C<sub>8</sub> films was also observed, retaining their shape in most commercially available organic solvents for up to 90 days (Fig. S10†). To further showcase the strong properties of the supramolecular HACS-SP-C<sub>8</sub> film, a car weighing over 1.8 tonnes can be pulled with the HACS-SP-C<sub>8</sub> film of 3 mm thickness as the connector (Fig. 2e and Movie S1†). The robust and stiff HACS-SP-C<sub>8</sub> film did not show any noticeable deformation, demonstrating eminent potential applicability.

### Remoldability and recyclability of supramolecular polyelectrolyte plastics

Strong plastics with high crosslinking densities are often extremely difficult to remold and recycle. The large plasticizers or modifiers are not able to penetrate due to the poor permeability of the dense network. The supramolecular HACS-SP-C<sub>8</sub> plastic is capable of achieving superior remoldability and recyclability by a combination of hydroplasticity and heating. The HACS-SP-C<sub>8</sub> film is stable under ambient conditions in water for over 150 days with only a slight swelling of the film (Fig. S11†). The multiple electrostatic crosslinking of the SP and the hydrophobicity of the *n*-octyl group sustain the network structure, which hinders the swelling of the network by water. Intriguingly, distinct shapes such as spiral, triangle, cylindrical, and S shapes of the film were successfully fabricated by immersing the original rectangular film into a water bath at 60 °C for 2 min (Fig. 3a). Upon drying, stiff polymeric materials with desired shapes were formed, displaying the outstanding remoldability of the supramolecular polyelectrolyte plastics.

Further, the same strategy is also feasible for the recyclability of the polyelectrolyte plastic (Fig. 3b). The HACS-SP-C<sub>8</sub> film was ground into thin powders, which can be hot-pressed (60 °C) into a new film in the presence of water. This process can be repeated several times in a straightforward fashion. The reclaimed films all manifest tensile strengths over 78.5 MPa and Young's moduli over 1.9 GPa, maintaining over 82% of the original mechanical properties (Fig. 3c and d). We suppose that water as the plasticizer is able to efficiently activate the cross-linked electrostatic network upon heating. Both the electrostatic crosslinking between SP and HACS and the hydrogen bonding of HACS can be disrupted upon heating in the presence of water, making the reorganization of the network possible. Collectively, dense hydrogen bonding and multiple electrostatic crosslinking within the polyelectrolyte plastic HACS-SP-C<sub>8</sub> enable us to remold and recycle the robust polymeric materials in a facile and environmentally friendly manner.

### Environmentally ion-dissociable supramolecular polyelectrolyte plastics

Most plastics with excellent mechanical properties require harsh catalytic or reaction conditions for degradation. Even for the

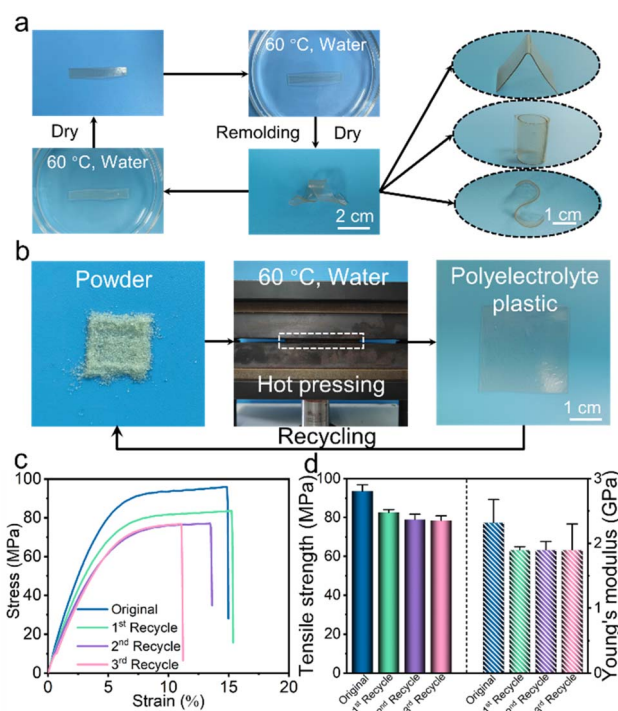
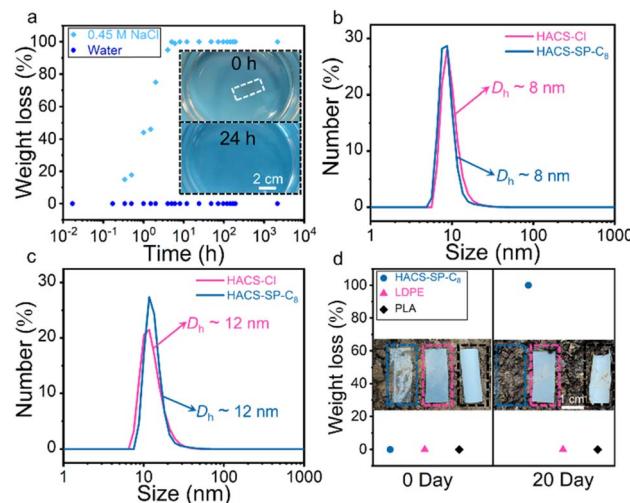


Fig. 3 Remoldability and recyclability of the supramolecular polyelectrolyte plastic HACS-SP-C<sub>8</sub>. (a) The remoldability of the supramolecular polyelectrolyte plastic HACS-SP-C<sub>8</sub> into different shapes upon heating using water as the plasticizer; (b) the recyclability of the supramolecular polyelectrolyte plastic HACS-SP-C<sub>8</sub> through a hot-pressing process; (c) representative stress–strain curves; and (d) mechanical properties of the original and recycled supramolecular polyelectrolyte plastic HACS-SP-C<sub>8</sub>.

typical biodegradable PLA, several studies indicate that no obvious signs of degradation of PLA were observed in seawater or soil for over at least 3 years.<sup>36–39</sup> Ambient conditions are not conducive to either surface degradation or bulk degradation of polyester materials. Additionally, the biodegradation of polymers with labile ester or ether bonds depends on the attack of enzymes, which is much faster for dispersed polymer chains than solid polymeric materials. Therefore, the efficient dissociation of bulk plastics provides a feasible way to avoid the pollution of discarded plastics. In order to get close to the salt concentration in seawater, we first chose the highest concentration of 0.45 M NaCl in seawater for research. As shown in Fig. 4a, the supramolecular polyelectrolyte plastic HACS-SP-C<sub>8</sub> has a weight loss of up to 95% at 5 h and no residual solids were observed at 24 h in 0.45 M NaCl solution. The inset of Fig. 4a shows the pictures of the HACS-SP-C<sub>8</sub> sample in the 0.45 M NaCl solution at 0 h and 24 h. In contrast, no organic substances were detected in aqueous solution after immersing HACS-SP-C<sub>8</sub> in water even over 150 days (Fig. 4a). High NaCl concentration weakens the electrostatic crosslinking and facilitates the counterion exchange to weaken the hydrophobic interactions, both of which disrupt the dense supramolecular network. As such, the robust supramolecular plastic is capable of efficiently dissociating in the NaCl solution under ambient conditions.

Dynamic light scattering (DLS) analyses were used to investigate the solution of the dissociated supramolecular





**Fig. 4** The dissociation of the supramolecular polyelectrolyte plastic HACS-SP-C<sub>8</sub>. (a) Weight loss of HACS-SP-C<sub>8</sub> with time in 0.45 M NaCl solution and water. The inset shows the pictures of the HACS-SP-C<sub>8</sub> sample in the 0.45 M NaCl solution at 0 h and 24 h; (b) DLS analyses of HACS-Cl and the dissociated HACS-SP-C<sub>8</sub> in 0.45 M NaCl solution, where the latter is measured after the dissociation of HACS-SP-C<sub>8</sub> in the NaCl solution for 24 h; (c) DLS analyses of HACS-Cl and the dissociated HACS-SP-C<sub>8</sub> in seawater, where the latter is measured after the dissociation of HACS-SP-C<sub>8</sub> in seawater for 72 h; (d) photos and weight loss of HACS-SP-C<sub>8</sub>, LDPE, and PLA before and after 20 days in natural soil.

polyelectrolyte film. The results show that a well-defined nano-object of  $\sim 8$  nm was found (Fig. 4b). The hydrodynamic diameter is close to that ( $\sim 8$  nm) of the HACS-Cl aqueous solution. Therefore, we surmise that the NaCl solution at high concentration is able to break down the supramolecular polyelectrolyte plastic HACS-SP-C<sub>8</sub> into its original components. Considering that lots of plastics accumulated in the ocean, we further evaluate the dissociation of the robust supramolecular polyelectrolyte plastic HACS-SP-C<sub>8</sub> in artificial seawater (Table S3 and Fig. S12 $\dagger$ ) and natural seawater (Fig. 4c). The results show that a well-defined nano-object of  $\sim 12$  nm was found for HACS-SP-C<sub>8</sub> in seawater (Fig. 4c). The hydrodynamic diameter is close to that ( $\sim 12$  nm) of HACS-Cl in seawater. Further, we analyzed the <sup>1</sup>H NMR of HACS-SP-C<sub>8</sub> after dissociation in seawater and measured the molecular weights of HACS-SP-C<sub>8</sub> after dissociation in artificial seawater and seawater. The results demonstrated that the dissociated chemical composition was the same as that of HACS-Cl, and the molecular weight of the dissociated HACS-SP-C<sub>8</sub> ( $M_w \sim 1.5 \times 10^5$  g mol<sup>-1</sup>) was similar to that of HACS-Cl ( $M_w \sim 1.5 \times 10^5$  g mol<sup>-1</sup>) (Fig. S13 and S14 $\dagger$ ). Some white precipitates observed during the dissociation were confirmed to be calcium phytate and magnesium phytate through FTIR and XPS analyses due to the presence of Mg<sup>2+</sup> and Ca<sup>2+</sup> in artificial seawater and natural seawater (Fig. S15–S17 $\dagger$ ). Further analysis of the white precipitates using relative mole ratios measured by XPS showed that 98% and 91% of the supramolecular polyelectrolyte plastic were dissociated into polymer chains in artificial seawater and natural seawater, respectively (Table S4 $\dagger$ ). At the same time, the degradation process of the non-ionically dissociable PLA was

further explored by directly immersing the plastic in seawater. The results show that the quantitative weight changes display no weight loss for PLA (Fig. S18 $\dagger$ ).

In addition to entering the ocean, a large volume of discarded plastics pollutes the soil and decreases the absorption of nutrients and moisture by crops, leading to a drop in crop production. The dissociation process of the supramolecular polyelectrolyte plastic HACS-SP-C<sub>8</sub> was further explored by directly burying the plastic in the outdoor soil (Fig. 4d). For comparison, PLA and low density PE (LDPE) films were also buried at the same position, 10 cm underground. Interestingly, the HACS-SP-C<sub>8</sub> polyelectrolyte film was completely dissociated in the soil, while neither PLA nor LDPE showed discernible changes. The quantitative weight changes also display no weight change for both PLA and LDPE (Fig. 4d). High moisture and various ions in the soil efficiently dissociate the robust and stiff polyelectrolyte plastic, which provides a new strategy to construct sustainable polymeric materials.

### Generalized strategy for fabricating environmentally ion-dissociable high-performance supramolecular polyelectrolyte plastics

The synergistic multivalent and hydrophobic counterion strategy provides a novel way to fabricate robust, remoldable, recyclable, and environmentally ion-dissociable polyelectrolyte plastics. To explore the generality of this approach, we substitute HACS-Cl with other bio-sourced and synthetic polyelectrolytes, such as cellulose 2-(2-hydroxy-3-(trimethylammonio)propoxy) ethyl ether chloride (CHTM-Cl) and poly(3-acrylamidopropyltrimethylammonium chloride) (PTMPA-Cl) (Fig. 5a and S19 $\dagger$ ). Specifically, the tensile strength of CHTM-SP-C<sub>12</sub> ( $84.9 \pm 3.3$  MPa) exceeds that of CHTM-SP ( $62.7 \pm 5.5$  MPa) and CHTM-C<sub>12</sub> ( $36.5 \pm 4.4$  MPa), demonstrating the synergy of multivalent and hydrophobic counterions considering the relative molar content of SP and C<sub>12</sub> in CHTM-SP-C<sub>12</sub> (Fig. 5b and c). Meanwhile, the Young's modulus of CHTM-SP-C<sub>12</sub> ( $2.3 \pm 0.3$  GPa) is significantly higher than that of CHTM-SP ( $1.6 \pm 0.6$  GPa) and CHTM-C<sub>12</sub> ( $0.8 \pm 0.1$  GPa), enabling the formation of stiff polymeric materials. Recyclability was also achieved for the stiff and strong polyelectrolyte plastic CHTM-SP-C<sub>12</sub> by grinding and hot-pressing the film with water as the plasticizer (Fig. 5d). The recycled plastic has similar tensile strength ( $81.7 \pm 13.8$  MPa) and Young's modulus ( $2.1 \pm 0.2$  GPa) to the original one (Fig. 5e and S20 $\dagger$ ).

Further study has indicated that the robust and stiff CHTM-SP-C<sub>12</sub> film can be dissociated in NaCl solution (0.45 M) under ambient conditions. DLS analyses show that the dissociated polymer in aqueous solution has a similar size to that of the original CHTM-Cl aqueous solution (Fig. 5f). For synthetic polyelectrolyte PTMPA-Cl, the combination of multivalent and hydrophobic counterions also gives rise to the formation of robust, recyclable, and environmentally ion-dissociable polyelectrolyte plastics (Fig. S21 and S22 $\dagger$ ), providing a universal approach for constructing high-performance eco-friendly plastics. It is expected that by combining various ions and plenty of polyelectrolytes, numerous sustainable high-performance plastics would emerge.

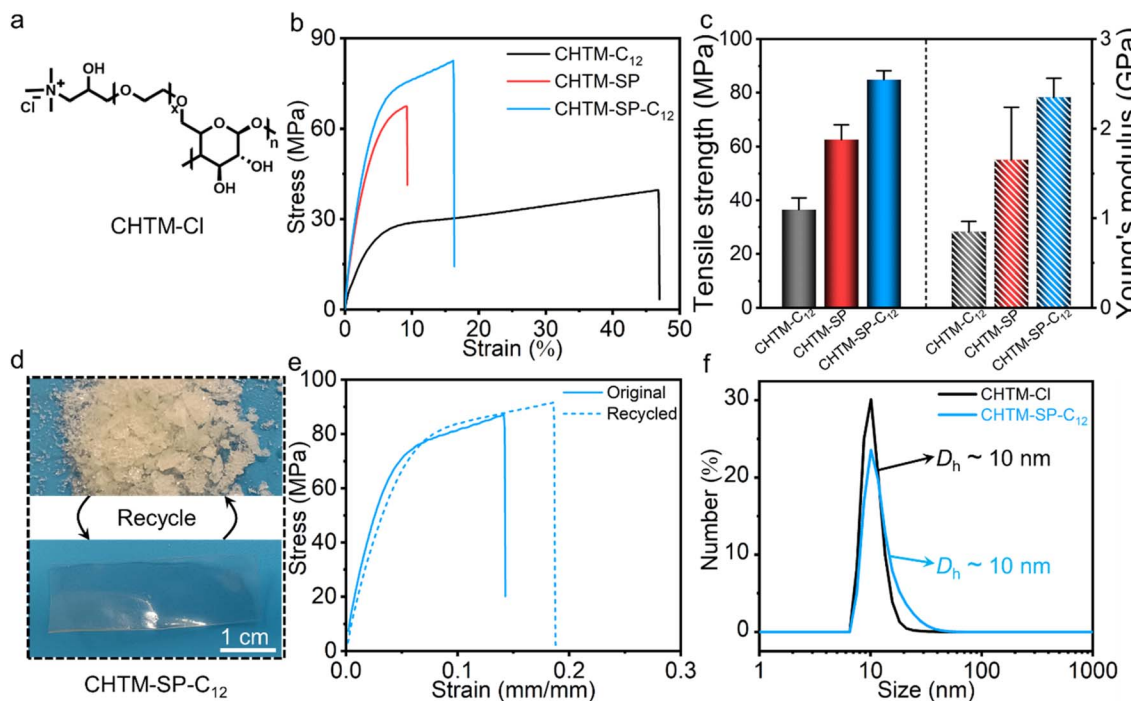


**Fig. 5** A universal approach for constructing stiff, recyclable, and ion-dissociable polyelectrolyte plastics. (a) Molecular structure of CHTM-Cl, (b) representative stress–strain curves and (c) mechanical properties of CHTM-C<sub>12</sub>, CHTM-SP, and CHTM-SP-C<sub>12</sub>. (d) Photos and (e) representative stress–strain curves showing the recyclability of CHTM-SP-C<sub>12</sub>. (f) DLS analyses of CHTM-Cl and the dissociated CHTM-SP-C<sub>12</sub> in 0.45 M NaCl solution, where the latter is measured after the dissociation of CHTM-SP-C<sub>12</sub> in NaCl solution for 24 h.

## Conclusions

In summary, we report a general strategy to fabricate environmentally ion-dissociable high-performance supramolecular polyelectrolyte plastics through the combination of multivalent and hydrophobic counterions. The multiple electrostatic crosslinking and hydrophobic interactions endow the supramolecular hydrogen bonding networks with good stability, high stiffness, and robustness. The optimized supramolecular polyelectrolyte plastic HACS-SP-C<sub>8</sub> has a tensile strength of  $93.6 \pm 3.3$  MPa and a Young's modulus of  $2.3 \pm 0.3$  GPa, outperforming most of the commercial plastics and polyelectrolyte plastics. Further, the supramolecular polyelectrolyte plastic can be remolded and recycled with water as the plasticizer upon heating in a facile manner. More importantly, efficient dissociation of the supramolecular polyelectrolyte plastic was achieved in the presence of environmentally associated ions in both seawater and soil. Finally, the simple fabrication strategy for the robust sustainable polyelectrolyte plastic appears to be applicable to other bio-sourced and synthetic polyelectrolytes based on the criteria developed herein. This work highlights the possibility of constructing sustainable high-performance plastics by rationally tailoring the supramolecular networks of polyelectrolytes.

## Data availability

The data that support the findings of this study are available in the ESI<sup>†</sup> of this article.

## Author contributions

The manuscript was written through contributions of all authors. All authors have given approval to the final version of the manuscript. Z. H. and G. L. designed the study. Z. D. carried out most of the experiments and analysed the related data. J. W. and A. L. participated in the experiments for polymer characterization.

## Conflicts of interest

The authors declare no competing financial interest.

## Acknowledgements

This work was financially supported by the National Natural Science Foundation of China (22273098, 22373003, 22103002, and 52033001) and the Key Project of Anhui Province Science and Technology Innovation Platform (No. 202305a12020030). Z. H. also acknowledged the financial support of Anhui Provincial Natural Science Foundation (No. 2408085Y004). This work was partially carried out at the Instruments Center for Physical Science, University of Science and Technology of China.

## References

- 1 K. Gong, L. Hou and P. Wu, Hydrogen-bonding affords sustainable plastics with ultrahigh robustness and

water-assisted arbitrarily shape engineering, *Adv. Mater.*, 2022, **34**, 2201065.

2 D. Li, Z. Han, Q. He, K. Yang, W. Sun, H. Liu, Y. Zhao, Z. Liu, C. Zong, H. Yang, Q. Guan and S. Yu, Ultrastrong, thermally stable, and food-safe seaweed-based structural material for tableware, *Adv. Mater.*, 2022, **35**, 2208098.

3 S. Choi, T. Kwon, A. Coskun and J. Cho, Highly elastic binders integrating polyrotaxanes for silicon microparticle anodes in lithium ion batteries, *Science*, 2017, **357**, 279–283.

4 R. Geyer, J. Jambeck and K. Law, Production, use, and fate of all plastics ever made, *Sci. Adv.*, 2017, **3**, e1700782.

5 P. Stegmann, V. Daioglou, M. Londo, D. P. van Vuuren and M. Junginger, Plastic futures and their CO<sub>2</sub> emissions, *Nature*, 2022, **612**, 272–276.

6 C. Jehanno, J. W. Alty, M. Roosen, S. De Meester, A. Dove, E. X. Chen, F. A. Leibfarth and H. Sardon, Critical advances and future opportunities in upcycling commodity polymers, *Nature*, 2022, **603**, 803–814.

7 M. MacLeod, H. Arp, M. Tekman and A. Jahnke, The global threat from plastic pollution, *Science*, 2021, **373**, 61–65.

8 M. C. Rillig, S. Kim and Y. Zhu, The soil plastisphere, *Nat. Rev. Microbiol.*, 2023, **22**, 64–74.

9 Y. Zhang, P. Wu, R. Xu, X. Wang, L. Lei, A. Schartup, Y. Peng, Q. Pang, X. Wang, L. Mai, R. Wang, H. Liu, X. Wang, A. Luijendijk, E. Chassagnet, X. Xu, H. Shen, S. Zheng and E. Y. Zeng, Plastic waste discharge to the global ocean constrained by seawater observations, *Nat. Commun.*, 2023, **14**, 1372.

10 Y. Zhao, E. Rettner, K. Harry, Z. Hu, J. Miscall, N. A. Rorrer and G. Miyake, Chemically recyclable polyolefin-like multiblock polymers, *Science*, 2023, **382**, 310–314.

11 G. Zhou, H. Zhang, Z. Su, X. Zhang, H. Zhou, L. Yu, C. Chen and X. Wang, A biodegradable, waterproof, and thermally processable cellulosic bioplastic enabled by dynamic covalent modification, *Adv. Mater.*, 2023, **35**, 2301398.

12 Y. Ma, X. Jiang, Z. Shi, J. A. Berrocal and C. Weder, Closed-loop recycling of vinylgous urethane vitrimers, *Angew. Chem., Int. Ed.*, 2023, **62**, e202306188.

13 G. Si, C. Li, M. Chen and C. Chen, Polymer multi-block and multi-block+ strategies for the upcycling of mixed polyolefins and other Plastics, *Angew. Chem., Int. Ed.*, 2023, **62**, e202311733.

14 L. Wimberger, G. Ng and C. Boyer, Light-driven polymer recycling to monomers and small molecules, *Nat. Commun.*, 2024, **15**, 2510.

15 X. Wu, P. Hartmann, D. Berne, M. Debruyne, F. Cuminet, Z. Wang, J. Zechner, A. Boese, V. Placet, S. Caillol and K. Barta, Closed-loop recyclability of a biomass-derived epoxy-amine thermoset by methanolysis, *Science*, 2024, **384**, 177.

16 K. Parkatzidis, H. S. Wang and A. Anastasaki, Photocatalytic upcycling and depolymerization of vinyl polymers, *Angew. Chem., Int. Ed.*, 2024, **63**, e202402436.

17 J. Rosenboom, R. Langer and G. Traverso, Bioplastics for a circular economy, *Nat. Rev. Mater.*, 2022, **7**, 117–137.

18 Y. Yu and M. Flury, Unlocking the potentials of biodegradable plastics with proper management and evaluation at environmentally relevant concentrations, *npj Mater. Sustain.*, 2024, **2**, 9.

19 E. T. Degens, Salts in the sea, *Nature*, 1973, **243**, 504–507.

20 J. Zhang, J. Zhu, Z. Hua and G.-M. Liu, Specific ion effects on the enzymatic degradation of polyester films, *Chin. J. Polym. Sci.*, 2022, **41**, 476–482.

21 K. Law, Plastics in the marine environment, *Annu. Rev. Mar. Sci.*, 2017, **9**, 205–229.

22 V. Nava, S. Chandra, J. Aherne, M. Alfonso, A. AntãoGeraldes, K. Attermeyer, R. Bao, M. Bartrons, S. Berger, M. Biernaczyk, R. Bissen, J. Brookes, D. Brown, M. CañedoArgüelles, M. Canle, C. Capelli, R. Carballeira, J. L. Cereijo, S. Chawchai, S. T. Christensen, K. S. Christoffersen, E. de Etyo, J. Delgado, T. N. Dornan, J. P. Doubek, J. Dusaucy, O. Erina, Z. Ersoy, H. Feuchtmayr, M. L. Frezzotti, S. Galafassi, D. Gateuille, V. Gonçalves, H. P. Grossart, D. P. Hamilton, T. D. Harris, K. Kangur, G. B. Kankılıç, R. Kessler, C. Kiel, E. M. Krynak, A. Leiva-Presa, F. Lepori, M. G. Matias, S.-i. S. Matsuzaki, Y. McElarney, B. Messyasz, M. Mitchell, M. C. Mlambro, S. N. Motitsoe, S. Nandini, V. Orlandi, C. Owens, D. Özkundakci, S. Pinnow, A. Pociecha, P. M. Raposeiro, E. I. Rööm, F. Rotta, N. Salmaso, S. S. S. Sarma, D. Sartirana, F. Scordo, C. Sibomana, D. Siewert, K. Stepanowska, Ü. N. Tavşanoğlu, M. Tereshina, J. Thompson, M. Tolotti, A. Valois, P. Verburg, B. Welsh, B. Wesolek, G. A. Weyhenmeyer, N. Wu, E. Zawisza, L. Zink and B. Leoni, Plastic debris in lakes and reservoirs, *Nature*, 2023, **619**, 317–322.

23 P. T. M. Albers, L. G. J. van der Ven, R. A. T. M. van Benthem, A. C. C. Esteves and G. de With, Water swelling behavior of poly(ethylene glycol)-based polyurethane networks, *Macromolecules*, 2020, **53**, 862–874.

24 C. Löwenberg, M. Balk, C. Wischke, M. Behl and A. Lendlein, Shape-memory hydrogels: Evolution of structural principles to enable shape switching of hydrophilic polymer networks, *Acc. Chem. Res.*, 2017, **50**, 723–732.

25 Y. Cheng, E. Hirano, H. Wang, M. Kuwayama, E. W. Meijer, H. Huang and T. Aida, Mechanically strong yet metabolizable supramolecular plastics by desalting upon phase separation, *Science*, 2024, **386**, 875–881.

26 Y. Yang, R. Xing, S. Liu, Y. Qin, K. Li, H. Yu and P. Li, Chitosan, hydroxypropyltrimethyl ammonium chloride chitosan and sulfated chitosan nanoparticles as adjuvants for inactivated Newcastle disease vaccine, *Carbohydr. Polym.*, 2020, **229**, 115423.

27 K. Collins, Ions from the Hofmeister series and osmolytes: effects on proteins in solution and in the crystallization process, *Methods*, 2004, **34**, 300–311.

28 N. Vlachy, B. Cwiklik, R. Vácha, D. Touraud, P. Jungwirth and W. Kunz, Hofmeister series and specific interactions of charged headgroups with aqueous ions, *Adv. Colloid Interface Sci.*, 2009, **146**, 42–47.

29 L. Liu, R. Kou and G. Liu, Ion specificities of artificial macromolecules, *Soft Matter*, 2017, **13**, 68–80.

30 M. Röttger, R. W. Trystan Domenech, A. Breuillac, R. Nicolaï and L. Leibler, High-performance vitrimers from commodity



thermoplastics through dioxaborolane metathesis, *Science*, 2017, **356**, 62–65.

31 D. G. Papageorgiou, I. A. Kinloch and R. J. Young, Hybrid multifunctional graphene/glass-fibre polypropylene composites, *Compos. Sci. Technol.*, 2016, **137**, 44–51.

32 H. Wang, G. Xie, Z. Ying, Y. Tong and Y. Zeng, Enhanced mechanical properties of multi-layer graphene filled poly(vinyl chloride) composite films, *J. Mater. Sci. Technol.*, 2015, **31**, 340–344.

33 M. K. M. Smith, D. M. Paleri, M. Abdelwahab, D. F. Mielewski, M. Misra and A. K. Mohanty, Sustainable composites from poly(3-hydroxybutyrate) (PHB) bioplastic and agave natural fibre, *Green Chem.*, 2020, **22**, 3906–3916.

34 G. Donald, A Literature Review of Poly(Lactic Acid), *J. Polym. Environ.*, 2002, **9**, 63.

35 J. Rosenboom, D. K. Hohl, P. Fleckenstein, G. Storti and M. Morbidelli, Bottle-grade polyethylene furanoate from ring-opening polymerisation of cyclic oligomers, *Nat. Commun.*, 2018, **9**, 2701.

36 G. Wang, D. Huang, J. Ji, C. Völker and F. R. Wurm, Seawater-degradable polymers—fighting the marine plastic pollution, *Adv. Sci.*, 2020, **8**, 2001121.

37 A. R. Bagheri, C. Laforsch, A. Greiner and S. Agarwal, Fate of so-called biodegradable polymers in seawater and freshwater, *Global Chall.*, 2017, **1**, 1700048.

38 A. Leduigou, A. Bourmaud, P. Davies and C. Baley, Long term immersion in natural seawater of Flax/PLA biocomposite, *Ocean Eng.*, 2014, **90**, 140–148.

39 T. Rheinberger, J. Wolfs, A. Paneth, H. Gojzewski, P. Paneth and F. R. Wurm, RNA-Inspired and accelerated degradation of polylactide in seawater, *J. Am. Chem. Soc.*, 2021, **143**, 16673–16681.

